Active vision via extremum seeking for robots in unstructured environments Applications in object recognition and manipulation

Calli, Berk; Caarls, Wouter; Wisse, Martijn; Jonker, Pieter P.

DOI
10.1109/TASE.2018.2807787

Publication date
2018

Document Version
Accepted author manuscript

Published in
IEEE Transactions on Automation Science and Engineering

Active Vision via Extremum Seeking for Robots in Unstructured Environments: Applications in Object Recognition and Manipulation

Berk Calli, *Member, IEEE,* Wouter Caarls, *Member, IEEE,* Martijn Wisse, *Member, IEEE,* and Pieter P. Jonker, *Member, IEEE*

***Abstract*— In this paper, a novel active vision strategy is proposed for optimizing the viewpoint of a robot's vision sensor for a given success criterion. The strategy is based on extremum seeking control (ESC), which introduces two main advantages: 1) Our approach is model free: It does not require an explicit objective function or any other task model to calculate the gradient direction for viewpoint optimization. This brings new possibilities for the use of active vision in unstructured environments, since *a priori* knowledge of the surroundings and the target objects is not required. 2) ESC conducts continuous optimization backed up with mechanisms to escape from local maxima. This enables an efficient execution of an active vision task. We demonstrate our approach with two applications in the object recognition and manipulation fields, where the model-free approach brings various benefits: for object recognition, our framework removes the dependence on offline training data for viewpoint optimization, and provides robustness of the system to occlusions and changing lighting conditions. In object manipulation, the model-free approach allows us to increase the success rate of a grasp synthesis algorithm without the need of an object model; the algorithm only uses continuous measurements of the objective value, i.e., the grasp quality. Our experiments show that continuous viewpoint optimization can efficiently increase the data quality for the underlying algorithm, while maintaining the robustness.**

***Note to Practitioners*—Vision sensors provide robots flexibility and robustness both in industrial and domestic settings by supplying required data to analyze the surroundings and the state of the task. However, the quality of these data can be very high or poor depending on the viewing angle of the vision sensor. For example, if the robot aims to recognize an object, images taken from certain angles (e.g., feature rich surfaces) can be more descriptive than the others, or if the robot's goal is to manipulate an object, observing it from a viewpoint that reveals easy-to-grasp "handles" makes the task simpler to execute. The algorithm presented in this paper aims to provide the robot high quality visual data relative to the task at hand by changing vision sensors' viewpoint. Different from other methods in the literature, our method does not require any task models (therefore, it is model free), and only utilizes a quality value that can be measured from the current viewpoint (e.g., object recognition success rate for the current image). The viewpoint of the sensor is changed continuously for increasing the quality value until the robot is confident enough about the success of the execution. We demonstrate the application of the algorithm in the object recognition and manipulation domains. Nevertheless, it can be applied to many other robotics tasks, where viewing angle of the scene affects the robot's performance.**

***Index Terms*— Active vision, extremum seeking control (ESC), object recognition, grasping, manipulation.**

Manuscript received July 27, 2017; revised November 7, 2017; accepted January 3, 2018. This paper was recommended for publication by Associate Editor H. Liu and Editor Y. Sun upon evaluation of the reviewers' comments. *(Corresponding author: Berk Calli.)*

B. Calli is with the Department of Mechanical Engineering and Materials Science, Yale University, New Haven, CT 06511 USA (e-mail: berk.calli@yale.edu).

W. Caarls is with the Department of Electrical Engineering, Pontifical Catholic University of Rio de Janeiro, Rio de Janeiro RJ 22451-900, Brazil (e-mail: wouter@caarls.org).

M. Wisse and P. P. Jonker are with the Department of Biomechanical Engineering, Delft University of Technology, 2628 CD Delft, The Netherlands (e-mail: m.wisse@tudelft.nl; p.p.jonker@tudelft.nl).

This paper has supplementary downloadable multimedia material available at http://ieeexplore.ieee.org provided by the authors. The Supplementary Material contains a video file displaying some examples of experiments presented in the paper. It gives two examples for each of the following. Active object recognition in non-occluded case. Active object recognition in occluded case. Active vision for grasp synthesis. This material is 11.0 MB in size.

Color versions of one or more of the figures in this paper are available online at http://ieeexplore.ieee.org.

Digital Object Identifier 10.1109/TASE.2018.2807787

I. Introduction

ACTIVE vision algorithms are utilized in robotics to supply better/more visual data for the execution of a given task by systematically changing the viewpoint and settings of the robot's sensor [1]. Especially in unstructured environments, these algorithms boost the abilities of robots by making them more robust to variations in data quality. They have various applications in object recognition [2], [3], saliency maximization [4], navigation [5], [6], object modeling [7], [8], and manipulation [9], where the vision sensor viewpoint affects the algorithm performance significantly.

In this paper, we propose a new viewpoint optimization methodology for increasing the efficiency and success rate of an underlying algorithm that utilizes the visual data. Our methodology is unique in the sense that it does not require an explicit objective function for viewpoint optimization; it maximizes a success criterion supplied by the underlying algorithm without the need of a task or environment model. This is achieved by adopting extremum seeking control (ESC) methods [10], which utilize the success criterion in a continuous optimization loop. The algorithms in the literature generally assume that the observation probability distribution is known given the action and current state (either being explicitly available, e.g., [2] and [11] or encoded via a learning process, e.g., [12] and [13]). In other words, these algorithms require a

decent estimate of the outcome for a given camera viewpoint even before visiting it. On the other hand, ESC algorithms do not require such knowledge (therefore are model-free) as they estimate the objective value gradient with continuous measurements and lead the camera accordingly.

Our model-free approach brings several advantages over the methods in the literature, especially for conducting viewpoint optimization in unstructured environments. We choose two domains in robotics to demonstrate and discuss these benefits: active object recognition and object manipulation. In the active object recognition, the duty of the active vision algorithm is to alter the sensor viewpoint for maximizing the recognition rate. The algorithms in the literature (e.g., [3] and [14]–[16]) rely on offline training data for conducting viewpoint optimization, which makes them sensitive to structured noise (e.g., occlusions, extreme lighting conditions). In addition, most of these algorithms employ discrete search techniques, and do not utilize the data between the way points. Our algorithm does not rely on offline training data for viewpoint optimization since it only uses the recognition rate value for continuous viewpoint optimization. In this way, robustness to structured noise is achieved while utilizing all the data acquired by the vision system in the optimization process.

In the object manipulation domain, the goal of the active vision system is to increase the success rate of grasp synthesis algorithms for grasping objects whose models are not available *a priori* (e.g., [17]–[21]). These algorithms utilize an image of the target object and aim to provide the poses of the robotic fingers on the object surface that achieve a successful grasp. In this case, the viewpoint optimization algorithm maximizes the quality of the grasp (therefore, its probability to be successful) by supplying better images of the object to the grasp synthesis algorithm. Compared to the active object recognition field, there are fewer strategies proposed for utilizing active vision for robotic manipulation. The majority of the strategies integrate viewpoint optimization into the manipulation pipeline, assuming that the object model is known, or a model is generated prior to manipulation (e.g., [22]–[24]). The methods for unknown objects in [25] and [26] boost the performance of a grasping algorithm by minimizing occlusions and measurement uncertainties, respectively. Our strategy, on the other hand, aids the grasp synthesis directly by providing images of the target object for which the algorithm is more confident in generating a good grasp. To the best of our knowledge, our methodology is the only one in the literature that can achieve this, thanks to its model-free nature.

Closest to our work, *Zhang et al.* [27] design an ESC algorithm for maximizing a saliency metric to help robots detecting interesting things in an environment. Nevertheless, experimental results are only presented for a single execution. In our work, we propose a general active vision methodology with an extensive experimental study.

In this paper, we first explain our ESC-based methodology in Section II. Following that, in Section III, we apply it to an active object recognition problem, discuss the advantages of our strategy in detail with respect to other algorithms in the literature, and present experimental validation. In Section IV, we apply the methodology to a grasp synthesis problem for unknown objects and also provide experimental evaluation. Section V provides the conclusion with discussions and future work.

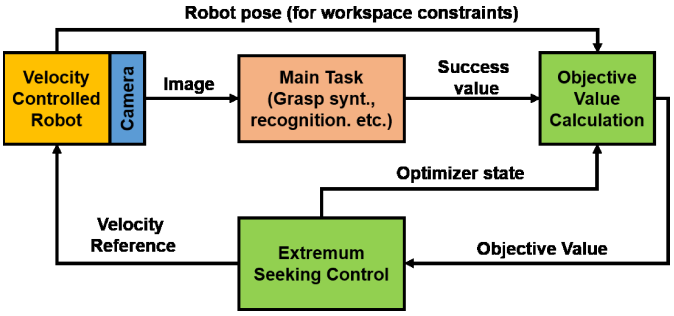

Fig. 1. Schema for the proposed ESC-based active vision methodology. The green blocks are for conducting viewpoint optimization and explained in depth in this paper.

II. Extremum Seeking Control-Based Active Vision

In our methodology, we use ESC optimizers [10] in a continuous viewpoint optimization loop. ESC algorithms address the problem of objective value optimization when the objective function, its gradient and the optimum value are unknown. They utilize the objective value continuously, estimate its gradient and supply a search direction accordingly. They also have mechanisms to avoid local optima (e.g., with hysteresis functions, in addition, for a strategy to further improve the global convergence performance of a particular ESC algorithm, the reader can refer to [28]). Some widely known applications of ESC are ignition time selection for combustion engines [29], bioreactor optimization [30], and anti-lock braking system control [31].

In the literature, there are four main types of continuous ESC algorithms: sliding mode ESC [32], neural network ESC (NN-ESC) [33], approximation-based ESC [34], and perturbation-based ESC [35]. The performance of these algorithms are compared in [10]. In this paper, we utilize NN-ESC as it is robust to objective value noise, and provides efficient results in multidimensional optimization problems. However, depending on the characteristics of the problem at hand, other ESC methods may also be preferable and can be used in the exact same methodology presented in this paper.

For our applications, the model-free nature of ESC algorithms (not requiring an explicit objective function) allows us to conduct viewpoint optimization without offline training or *a priori* information about the task or the target object. The application specific advantages of the method will be covered in detail in Sections III and IV.

A general overview of our method can be seen from Fig. 1. Here, an image is captured by the robot's camera and supplied to the target algorithm, which would benefit from viewpoint optimization (e.g., object recognition, grasp synthesis). The algorithm processes this image and generates a success rate value (e.g., probability of recognizing an object, the quality

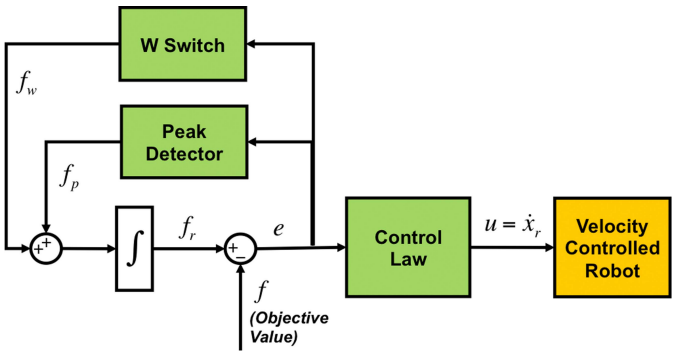

Fig. 2. Block diagram of NN ESC. It is one of the options for the ESC block in Fig. 1. We utilized NN ESC in our active object recognition and manipulation implementations due to its efficiency and robustness to objective value noise.

of the best grasp for the given data). The success rate forms the main component of the objective value, which is aimed to be maximized by the ESC algorithm. It can also be combined with workspace and optimizer specific constraints for improving safety and efficiency of the operation. The resulting objective value is utilized by the ESC algorithm and converted into velocity references for the robot. The robot moves with these references and a new image is captured from the sensor. The process continues until the objective value is above a certain threshold. In our experiments, this loop is run in 7 and 10 Hz. Like many active vision systems in the literature (e.g., [12], [15] and [36]), we also move the camera on a viewsphere, i.e., camera pointing to the object all the time while keeping the distance fixed; our NN-ESC algorithm provides a 2-D velocity vector that is always tangential to the viewsphere. Nevertheless, the proposed scheme can be used without a view sphere, with fewer or more motion constraints. The 2-D NN-ESC is designed as follows.

A. 2-D Neural Network ESC

The block diagram of NN-ESC can be seen from Fig. 2. The algorithm generates its own reference f_r by using the peak detector and the W switch

$$f_r = f_p + f_w \tag{1}$$

where f_p and f_w are the outputs of the peak detector and W switch, respectively. These switches use the error obtained by the difference between the current objective value and the reference value

$$e = f_r - f. \tag{2}$$

As the algorithm is initialized with the initial objective value ($f_r = f$), the W switch is not active; the only contribution to the f_r value comes from the peak detector. The switching mechanism of the peak detector is as follows:

$$\dot{f}_p = \begin{cases} M, & (e < 0) \\ 0, & (e \geq 0) \end{cases} \tag{3}$$

where M is a positive constant. By this mechanism, the peak detector converges to the value of the maximum objective value that is measured during the process. In order to maintain this convergence, the rate of change of the objective value should be smaller than M

$$|\dot{f}| < M. \tag{4}$$

The control law u, which is fed to the robot as velocity reference, tries to minimize the error by the following switching functions with hysteresis:

$$u_1 = \begin{cases} -U, & e < -\delta_1 \\ U, & e > \delta_1 \\ [\text{previous\_state}], & \text{otherwise} \end{cases} \tag{5}$$

$$u_2 = \begin{cases} 0, & e < -\delta_2 \\ -U, & e > \delta_2 \\ [\text{previous\_state}], & \text{otherwise} \end{cases} \tag{6}$$

$$u_3 = \begin{cases} 0, & e < -\delta_3 \\ 2U, & e > \delta_3 \\ [\text{previous\_state}], & \text{otherwise} \end{cases} \tag{7}$$

$$u = \begin{bmatrix} u_1 + u_2 \\ u_2 + u_3 \end{bmatrix}. \tag{8}$$

Here, U is a constant that specifies the magnitude of the velocity reference, and δ_i are the hysteresis widths. The control law is initialized with the following values:

$$(u_1, u_2, u_3) = (-U, 0, 0). \tag{9}$$

The switching mechanism of the control law works as follows: if the direction of the system makes the objective value converge to the optimum value, then this direction is kept. Otherwise, the error will increase, and when it is greater than the hysteresis values, the direction will be changed. This nested structure of hysteresis functions brings the following constraint to the hysteresis widths:

$$\delta_1 < \delta_2 < \delta_3. \tag{10}$$

When e becomes greater than δ_3, the control law enters its last state. This state ends as the error is larger than the threshold Δ where

$$\Delta > \delta_3. \tag{11}$$

As the Δ threshold is exceeded, the reference value f_r should be reset, so that a new cycle can start. The f_w function performs this by the following switching function:

$$\dot{f}_w = \begin{cases} -W, & e > \Delta \\ 0, & e < -\Delta \\ [previous\_state], & \text{otherwise} \end{cases} \tag{12}$$

where W is a positive constant. By this function, when the error is greater than the Δ threshold, the f_r will decrease until the error is less than $-\Delta$. This makes the control law go back to its first state.

The control signal u is fed to the systems as velocity input

$$\dot{x}_r = u. \tag{13}$$

While applying an NN ESC algorithm, the parameters are needed to be tuned considering the noise on the objective value

and the hysteresis that is wished to be allowed to escape from local minima.

In the next section, a way of forming the objective value within the framework is explained.

B. Objective Value Calculation

The success rate of the underlying algorithm form the main component of the objective value that is aimed to be maximized. Nonetheless, we add two other components to impose workspace constraints and to make the optimization process more efficient as follows. The objective value is defined as

$$f(v, r_s, w_s, x_o) = f_g(v) + f_s(r_s, w_s) + f_o(o_s) \qquad (14)$$

where v is the success rate value, r_s is the pose of the robot, w_s are the workspace constraints, o_s is the state of the optimizer, and f_g, f_s, and f_o are the success rate, workspace and optimizer specific components, respectively. f_g is calculated specific to the algorithm, and examples of its design will be covered for object recognition and manipulation in the Sections III and IV, respectively. The workspace constraints component is defined as a barrier function [37] as follows:

$$f_s(r_s, w_s) = \mu_w \sum_{n=1}^{k} \ln(r_{sn} - w_{sn}). \qquad (15)$$

Here, μ_w is the barrier parameter, k is the number of degrees of freedom of the robot, and r_{sn} and w_{sn} are the components of the robot's state vector and the workspace constraints. This function drops rapidly as the robot approaches to the close vicinity of the workspace constraints. This makes the objective value violate hysteresis values of the NN-ESC and forces it to change direction.

The optimizer specific component aids the NN-ESC algorithm as follows: while conducting viewpoint optimization, the NN-ESC can get into a direction that has a relatively small gradient. If the gradient is negative, the camera will need to travel long distances before the hysteresis thresholds of the NN-ESC algorithm are violated. For these cases, imposing a time constraint via a barrier function helps to increase the efficiency

$$f_o(o_s) = \mu_o \ln(\tau_o - \tau_p(o_s)). \qquad (16)$$

In (16), τ_p is the elapsed time since the maximum value of f_g is measured in the current state of the optimizer. The value of this component will drop rapidly as the state of the optimizer does not cause the objective value to increase until the allowed time τ_o. This will act as a penalty component in the objective function, and the state change for the viewpoint optimizer will be triggered. μ_o is the barrier parameter of this component.

In the next two sections, we present the application of our methodology to object recognition and grasp synthesis fields, respectively. The advantages of adopting the proposed strategy are given in detail.

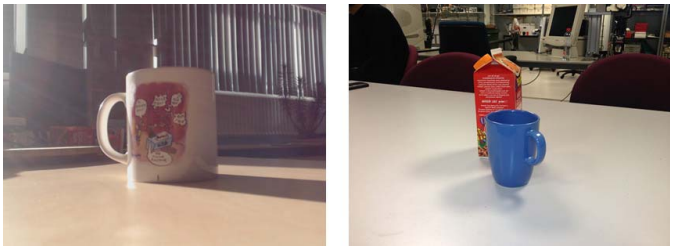

Fig. 3. Examples of structured noise which are very common in daily environments. An example of extreme lighting conditions (left) and an example of an occlusion (right).

III. Viewpoint Optimization for Object Recognition

Object recognition is one of the core necessities for robots as it enables them to locate target objects in a map [38], fetch requested objects for the user [39], use predefined strategies for manipulation [40], and draw some conclusions about the environment based on the recognized objects [41] among many other tasks. The sensor viewpoint is an essential factor that affects the performance of a recognition algorithm as some viewpoints of the object are more descriptive than some others. Active object recognition algorithms aim to optimize the sensor viewpoint to boost the success rate of the object recognition methods. These algorithms are especially crucial for robots operating in unstructured environments, since very few assumptions can be made on the initial viewpoint of the robot's sensor. In addition, the utilized active vision strategy should be robust to occlusions and changing/extreme lighting conditions, which are ubiquitous in unstructured environments and affect the performance of a recognition algorithm significantly (see Figs. 3 and 4).

Various solutions have been proposed for the active object recognition problem. A comprehensive list and comparison of active recognition algorithms can be found in [1], [42], and [43]. One of the common solutions in the literature is next best view selection by increasing the mutual information [2], [14], [44]. By this approach, planning the next viewpoint is conducted by searching the whole action space for the maximum object class and observation mutuality, considering the previous actions and observations. Another common approach is increasing the discriminative information among the class predictions by entropy minimization [11], [15]. In [12], flow images are generated offline in order to provide motion references to the system for minimizing the entropy. Learning techniques are also utilized, in which a policy that maps states to actions is learned for increasing the discriminative information. A very common way of learning this policy is via reinforcement learning algorithms [3], [14], [16], [45]–[49]. In addition to these methods, a feature space trajectory representation is presented in [13]. By this representation, the most discriminative viewpoints are computed in an offline manner. Also, a rule-based method is presented in [50], where the recognition system is trained for recognizing Fourier Descriptor based models of the object silhouette. In this method, the next viewpoint is

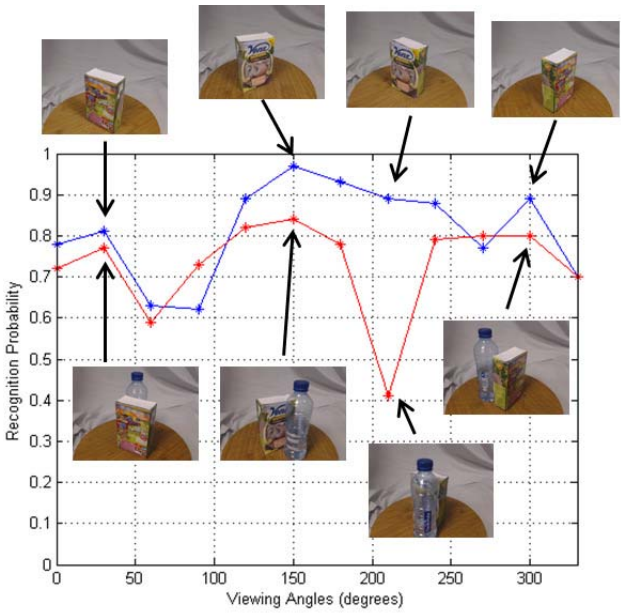

Fig. 4. Effect of occlusion on object recognition success: recognition probability of an object is given for various viewing angles as it is the only object in the scene (blue line), and while it was occluded by an object outside the training data set. It can be seen that occlusion affects the recognition rate dramatically.

selected based on some heuristics assuming that the object is not occluded.

In the next section, we discuss the advantages of our proposed methodology over the abovementioned algorithms.

A. Advantages of the Proposed Strategy

The active object recognition algorithms in the literature rely on offline training data, which make it harder to maintain robustness for the cases that the data cannot capture the current situation. On the other hand, the model-free active vision strategy proposed in this paper does not utilize training data and conducts continuous viewpoint optimization that can adapt/respond to the current state of the environment. Therefore, while the algorithms in the literature suffer from structured noise, the inefficiency caused by discrete search and imperfect training data, the proposed approach maintains system robustness. These points are detailed as follows.

1) Effect of Structured Noise: The methods in the literature rely on offline information that is mostly assumed to be obtained in the training phase: In all these cases, it is assumed that the observation probability distribution is known for a given action and current class belief. More specifically, if an action, an observation and an object class are denoted by a, o, and c, these algorithms need to know the probability distribution $P(o|c,a)$ in order to decide on the next action (the way that this decision is made varies depending on the algorithm). The learning-based methods and offline methods like [12] and [13] do not explicitly need this information in the decision phase, but it is encoded in the policy that is learned during the training process. Knowing $P(o|c,a)$ implies that, given the class of the object that we are looking for, we need to know what kind of measurement that we are going to have, if we take action a. This information can be obtained from position-labeled off-line training images. However, counting on this observation probability distribution for selecting an action relies on a very strong assumption: the data that is acquired offline should be valid for the current environmental conditions. In other words, if the system does not see what it expects to see in the destination viewpoint, this will affect the belief distribution on object class, and the system will tend to believe that the initial reasoning about the object class and pose was wrong. However, unexpected observations at the destination viewpoint may occur due to the occlusions, extreme lighting conditions or any kind of structured noise.

One of the rare active object recognition systems that address the occlusion problem is presented in [51], where a solution is provided by adding synthetically occluded images of the objects to the training data set. However, such a system can only be robust to the trained occlusions. Moreover, their system includes a turntable and two movable cameras with 90° viewing angle difference, which makes the job of the algorithm much easier compared to many realistic robotics scenarios. In addition to that work, a method for calculating a visibility metric for a given viewpoint is proposed in [52], which is aimed to be utilized in cluttered environments, but is not integrated to any viewpoint selection strategy.

2) Inefficiency Caused by Discrete Search: Another disadvantage of the presented active object recognition methods is that, while moving to the next best viewpoint, the data that can be acquired on the way to the destination is not used. However, utilization of this data can be very useful in reducing the execution time of the algorithms.

Very few algorithms use the data continuously in the active recognition literature. Huber *et al.* [2] and Eidenberger and Scharinger [53] use continuous viewpoint space, but the resultant decisions are discrete, so they do not utilize the data on the way to the destination. Robbel and Roy [54] use Fourier descriptors to model the silhouette of the object and recognize the object by the continuous change of the modeled shape. Although successful and efficient results are obtained by this method, the algorithm is vulnerable to acquired shape changes due to occlusions. A recent work in [47] acknowledges the importance of utilizing the data between way points and optimizes the camera trajectory to benefit from these data. Nevertheless, their viewpoint optimization strategy is not designed to handle structured noise-related issues that are explained in Section III-A1.

3) Effect of Imperfect Training Data: Using training images for selecting the next best viewpoint may be problematic when the training images are not taken in laboratory conditions. Two common cases are using object images from internet search [55], [56] and a robot learning a new object [57]. This causes a problem that is analogous to the one explained in Section III-A1, but this time it is caused by the training data. Moreover, in the case of obtaining images from the Internet, the relative pose of the camera with respect to the object is unknown. This makes the effect of the action on the current state impossible to calculate, since the current state and the

states of the other online images cannot be known. As a result, the reasoning process of the abovementioned active object recognition algorithms becomes inapplicable.

The implementation using our algorithm presented in the next section does not rely on any offline data and it conducts a continuous viewpoint optimization. Therefore, the advantages caused by imperfect training data and discrete search are avoided.

B. Implementation and Experiments

In this section, we present an implementation of our methodology to the active object recognition problem. We first explain the utilized object recognition algorithm followed by the description of our experimental setup and the experimental results with and without structured noise.

1) Object Recognition: For object recognition, we chose to use the bag of features method [58], since it is a commonly used algorithm in the literature and its advantages and drawbacks are well known. Nonetheless, it is important to note that the active vision strategy proposed in this paper can be used by any other object recognition method which outputs a recognition rate value. The features are detected using speeded up robust features descriptors, and each object in the training set is trained with a one-vs-all scheme via a support vector machine (SVM) using a radial basis function as kernel. In the classification phase, SVM provides signed distances to the separating hyperplane for each object. These distances are converted to probabilities by fitting sigmoid functions using Platt scaling [59]. The parameters of the scaling are obtained by a separate training image set of each object. The probabilities of each class are then compared to find the most probable class. We would like to clarify that the training here is solely for the object recognition algorithm, and no training phase or training images are necessary for the viewpoint optimization purposes unlike the abovementioned methods in the literature.

For calculating the f_g component of (14), we directly use the distance to the separating hyperplane of the most probable class instead of using the classification probability values that are obtained by Platt scaling. There are mainly two reasons for this choice: First, the sigmoids fit by Platt scaling saturate at both ends of the curve which affects the optimizer's performance; very small changes are observed at the saturated regions which does not provide information that is rich enough for the optimization. Also, in the nonsaturated regions, the increase in the recognition value may be too sudden and steep due to the scaling which also affects the performance of the optimizer negatively. Moreover, the scaling parameters that are obtained by the fitting process are dependent on the quality of the training image set, which we would like to avoid. On the other hand, by minimizing the distance to the separating hyperplane, we are able to optimize the recognition performance regardless to the scaling quality. This choice is validated by our preliminary experiments.

2) Experimental Setup: Our experimental setup is made up of a UR5 type Universal Robots arm, a webcam attached to the end-effector of the robot and a rotating platform (Fig. 5).

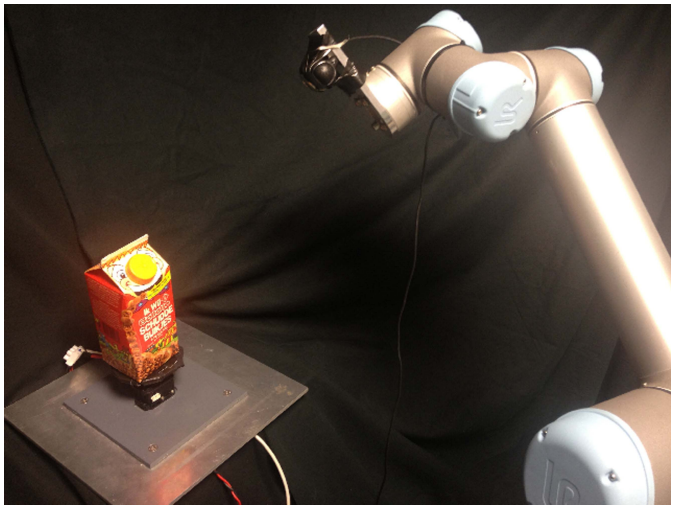

Fig. 5. Experimental setup: The UR5 type robot arm, the webcam attached to the tooltip of the robot, and the rotating platform.

Fig. 6. Objects that are used in the experiments.

We have trained the object recognition algorithm with twelve different objects, which can be seen from Fig. 6.

The performance of the algorithm is tested with and without occlusion for each object. For both cases, six experiments are conducted per object with 60° rotation difference (introduced by the rotating platform), 144 experiments in total. The optimization loop is run at 7 Hz. For each run, the initial velocity of the robot is selected randomly, and the NN-ESC algorithm is activated. If the most probable class changes during the operation, the optimizer is restarted. In order to avoid rapid switching of the most probable class, a low pass filter is applied to the class probabilities. The parameters of the NN-ESC are selected as $U = 0.02$, $\delta_1 = 0.08$, $\delta_2 = 0.11$, $\delta_3 = 0.14$, $\Delta = 0.17$, $M = 0.2$, and $W = 0.5$.

An experiment is considered successful, if the algorithm can increase the recognition probability of the correct object up to 95%. If this success rate cannot be achieved within 30 s, the process is terminated, and the most probable class

TABLE I

SUMMARY OF THE 144 EXPERIMENTS: SUCCESS RATE AND AVERAGE EXECUTION TIME OF THE ALGORITHM WITH AND WITHOUT OCCLUSION FOR DIFFERENT TERMINATION LEVELS

		Success	Avg. time (s)
3w/o occlu.	Initial view	36.1%	
	Reached %95 (ESC)	91.6%	9.4
	Terminated after 30 s (ESC)	95.8%	
3w/ occlu.	Initial view	36.1 %	
	Reached %95 (ESC)	83.3%	10.4
	Terminated after 30 s. (ESC)	97.2%	

(a)

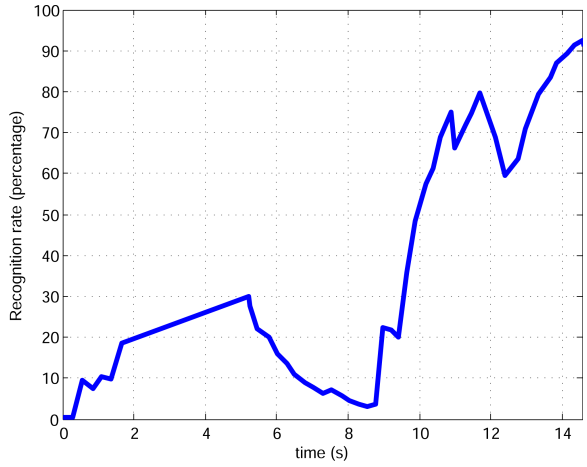

(b)

Fig. 7. Experimental results with "hagel slag" box. (a) Snapshots from an experiment without occlusion. Initial view (left). Final view (right). (b) Recognition probability versus time. The recognition rate increases over time and hits 95%.

in the overall trajectory is considered as the final guess of the algorithm (results are presented separately).

3) Experimental Results: All the experimental results are summarized in Table I. For the experiments without occlusions, the object is correctly recognized directly from the initial view (before active vision is initiated) with 95% recognition rate for 36.1% of the cases. For the other cases, when the proposed active recognition algorithm is run, 95% recognition rate is achieved by changing the viewpoint of the camera

(a)

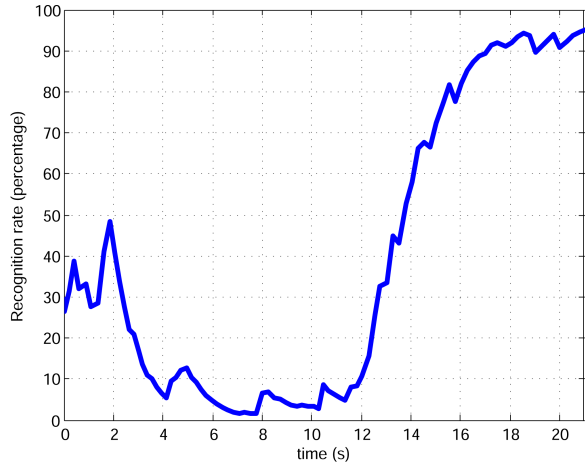

(b)

Fig. 8. Experimental results with "rice dream" box. (a) Snapshots from an experiment without occlusion. Initial view (left). Final view (right). (b) Recognition probability versus time. The recognition rate increases over time and hits 95%.

via ESC algorithm, and the success rate increases to 91.6%. For the 4.2% of the cases, the algorithm fails to reach 95% recognition rate in 30 s, and the algorithm is terminated. However, the most probable class is still correct at the end of the process (which sums up to 95.8% success). For the other 4.2% of the cases, the object is guessed wrong as the highest measured probability during the process belongs to a wrong object.

Two samples from the experiments are presented in Figs. 7 and 8. When the distance to the separation hyperplane is raised above the hysteresis threshold values, the ESC algorithm changes velocity reference and forces the distance to decrease. This causes an increase in the recognition rate of the object and 95% recognition rate is achieved eventually. The average time of obtaining the correct guess is 9.4 s.

In order to evaluate the performance of the algorithm under structured noise, occlusion is applied. As the results are compared with the nonoccluded case, the significant difference appears to be the decrease while obtaining 95% recognition rate. Although the object is guessed correctly in 97.2% of the cases, the recognition rate cannot be raised to 95% in some

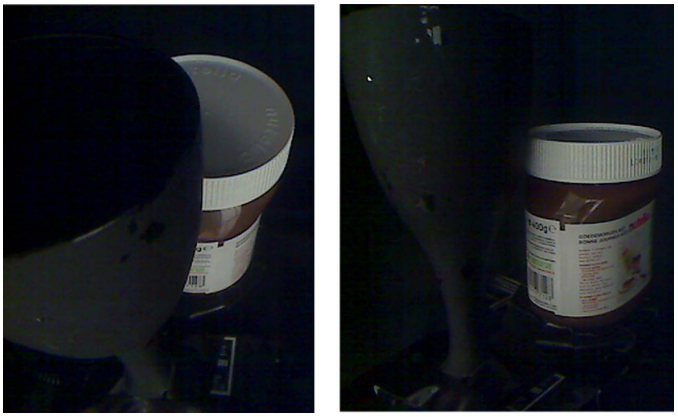

(a)

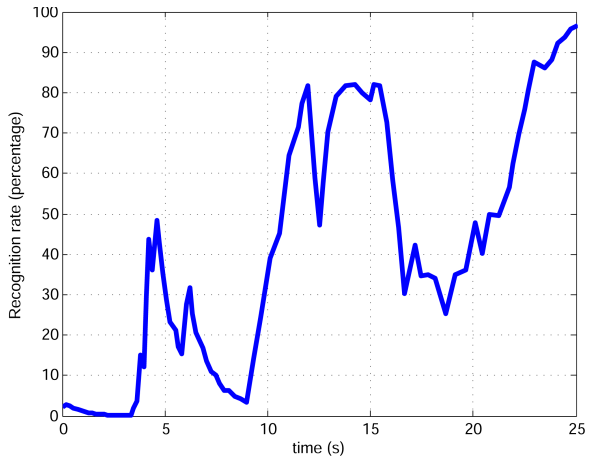

(b)

Fig. 9. Experimental results with "nutella" jar. (a) Snapshots from an experiment with occlusion. Initial view (left). Final view (right). (b) Recognition probability versus time. The recognition rate increases over time and hits 95%.

(a)

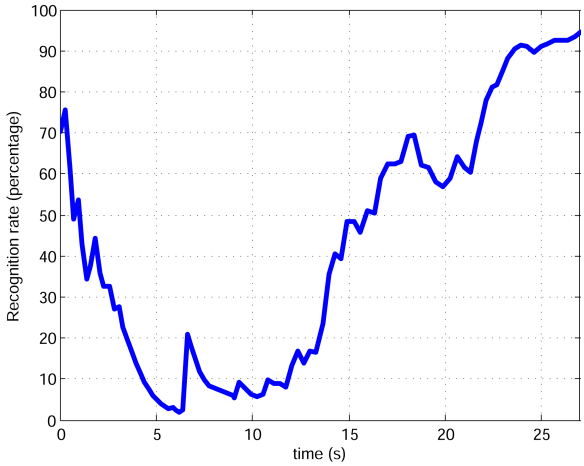

(b)

Fig. 10. Experimental results with "ruijer" box. (a) Snapshots from an experiment with occlusion. Initial view (left). Final view (right). (b) Recognition probability versus time. The recognition rate increases over time and hits 95%.

runs due to the occluded regions of the object. Also, a slight increase in average convergence time is observed since it takes more time to find a good viewpoint due to occlusions.

Two samples from the experiments with occlusion are given in Figs. 9 and 10. As can be seen from Figs. 9 and 10, the algorithm successfully avoid occlusions and leads the robot to a good viewpoint for recognition. However, the process takes more time and the recognition rate varies more than the nonoccluded case. These large variations are due to the steep scaled values, and might have been a problem for the ESC algorithm, however, thanks to the better-behaved hyperplane distance that we used in the optimization process, the algorithm is able to optimize the viewpoint successfully in the majority of the cases (as explained in Section III-B1).

For the cases in which the algorithm fails to recognize the object, it is observed that the algorithm gets stuck in a region where the number of features is low. As a result, a healthy guess cannot be made by the recognition algorithm, and the optimizer cannot go out of local maxima and fails.

Next, we present the application of our active vision methodology for the grasp synthesis problem.

IV. Viewpoint Optimization for Grasp Synthesis

In unstructured environments, the model of the target object is usually unavailable to the robot prior to manipulation. Therefore, grasp synthesis algorithms need to rely on the incomplete information acquired by their vision sensors while deciding on a grasping strategy. The algorithms in the literature generally optimize a grasp using one single image of the target object either using learning methods [17]–[19], [60] or heuristics [20], [21]. The fact that they synthesize a grasp using a single viewpoint makes the pose of the object with respect to the sensor a crucial factor: When the object is observed from a "good" viewpoint (which can be different for each method and object), these algorithms provide a very high success rate for a huge variety of objects. However, for many other viewpoints, the success rates of the algorithms drop significantly. This problem can be solved by utilizing an active vision strategy. As it is indicated by Spaan [61], this kind of visual exploration is a crucial element in order to fill the gap between neuroscience models and robotic implementations of grasping.

Most grasp synthesis algorithms have an internal optimization process in order to synthesize the best grasp with the

data at hand; for a given single image, they utilize a grasp quality metric and maximize it by changing the grasping pose. The goal of the viewpoint optimization in this case is to maximize the grasp quality by changing the viewpoint of the sensor and supplying "better" images to the grasp synthesis algorithm. The definition of a "better" image naturally depends on the grasp synthesis algorithm. Nevertheless, our method does not require any information about how the grasp synthesis algorithm works; it treats the algorithm as a black box and only utilizes the grasp quality value.

In the manipulation literature, active vision is often utilized for known object models [22], [23]. In this case, the role of viewpoint optimization is to localize the target object. In [24], a complete 3-D model of the object is generated prior to manipulation. On the other hand, very few works utilize active vision for grasping unknown objects. In [26], active vision is used to refine the surface reconstruction of the grasp location candidates, which results in a more reliable grasp execution. Kahn *et al.* [25] address the problem of grasping unknown objects in the presence of occlusion. In this case, the active vision system aims to minimize occlusions on the grasp handles of the objects. Similar to our case, this approach also uses a local optimizer that generates continuous trajectories rather than selecting discrete next best views. Nevertheless, their approach is specifically designed for scenarios with occlusions.

Our methodology, being the only model-free approach applied to object manipulation, aids the grasp synthesis algorithm directly by supplying better views: since the model of the object is unknown, the objective function based on the grasp quality cannot be calculated for an unvisited viewpoint. From the optimization perspective, this means the objective function that we want to optimize is unknown. Moreover, the gradient of this function is not calculable or cannot be measured directly. We can only calculate the value of the objective function for our current state, or in other words, our objective value. Our method utilizes this value for viewpoint optimization, and does not require an objective function. The next section presents our implementation and experimental results.

A. Implementation and Experiments

Within the abovementioned framework, for grasp synthesis, we used a silhouette-based algorithm in which the grasping point locations are optimized on a parametric model of the silhouette contour considering force closure and curvature of the contact surface (maximizing concavity) based on the method presented in [62]. In a nutshell, the silhouette of the object is segmented and modeled using elliptic Fourier descriptors. By taking the first and second derivatives of these parametric models, explicit equations can be obtained for calculating tangent and normal vectors for a given point on the contour. These expressions are used to optimize curvature values and force application directions. The algorithm searches for the grasping point locations that exhibit maximum concavity, while also satisfying the force closure property. Therefore, for this algorithm, the quality of the grasp is measured by the sum of curvature of the stable grasping points, and this measure is optimized to find the best grasp.

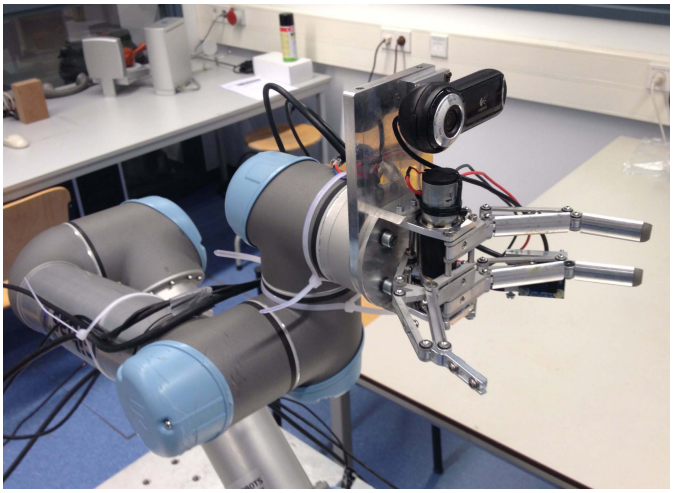

Fig. 11. Eye-in-hand system formed with a UR5 type universal robot arm, a Delft Hand 3 gripper, and a Logitech webcam.

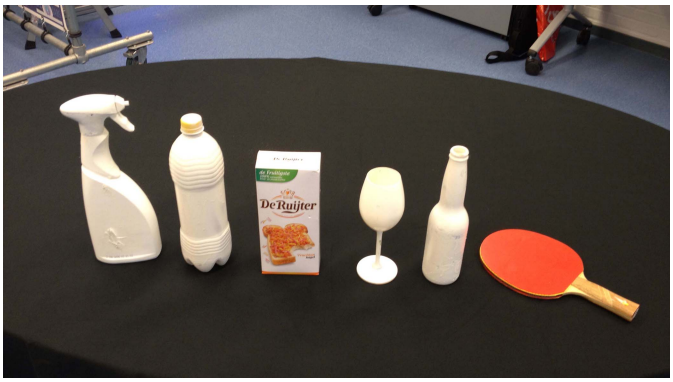

Fig. 12. Objects used in the experiments. From left to right: a spray bottle, a water bottle, a box, a wine glass, a beer bottle, and a table tennis racket.

For viewpoint optimization, the quality value of the best grasp that is synthesized using the last captured image is used as the f_g value of (14), and combined with workspace and optimizer specific components as explained in Section II-B. Similar to the active object recognition case, our methodology can also be utilized with any other grasp synthesis algorithm that can output a grasp quality value.

The experiments are conducted using the same UR5 setup with an addition of the Delft Hand 3 gripper [63] attached to the end-effector of the robot (Fig. 11). This gripper can apply a power grasp as well as a precision grasp. A distance sensor, which is used to close the gripper when the object is close enough, is placed at the palm of the gripper.

Six household objects in Fig. 12 are positioned in front of the robot with three different orientations, and the robot is initialized in two different poses as presented in Fig. 13 (six experiments per object). The viewpoint optimization is terminated after one full circle of NN-ESC (when W threshold is exceeded). This last pose of the gripper is the approach vector, as the gripper follows a straight line toward the object and closes when the grasping distance is achieved. The distance threshold is set to power grasp for all the objects except for the table tennis racket. Note that with the chosen grasp

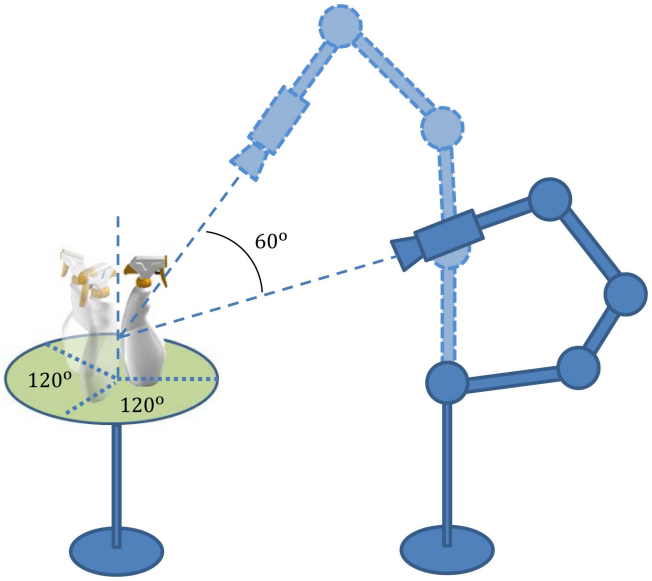

Fig. 13. Illustration of the experiments: The three different orientations for the object with 120 ° rotation difference and two different initial positions of the robot, which have 60 ° rotation difference around the x-axes of the camera frame.

TABLE II
SUMMARY OF THE EXPERIMENTAL RESULTS FOR THE GRASPING SCENARIO

Object Name	Successful Exp. / Total Exp.
Box	6/6
Spray Bottle	5/6
Glass	2/2
Tennis Racket	2/6
Beer Bottle	2/2
Water Bottle	2/2
Total	19/24

synthesis algorithm the robot fails to grasp these objects with its initial approach vector prior to the viewpoint optimization (this algorithm conducts 2-D grasp synthesis since it utilizes object silhouettes; using the viewpoint optimization algorithm effectively makes it suitable for 3-D applications). The parameters of the NN-ESC are selected as $U = 0.02$, $\delta_1 = 0.15$, $\delta_2 = 0.2$, $\delta_3 = 0.25$, $\Delta = 0.3$, $M = 0.2$, and $W = 0.7$.

The results are summarized in Table II, and object initial and final poses are presented in Fig. 14. In all the experiments, the viewpoint optimization was successful in increasing the viewpoint quality with respect to the given measures, i.e., force closure and model curvature. This aids the grasp synthesis algorithm since the grasping points are placed to much better locations on the object. The new viewpoints are also better approach vectors for grasping. These advantages bring successful grasps for the box, wine glass, beer bottle, and water bottle for all different initial viewpoints. For the spray bottle, only one initial view is failed. This makes up 94% success for the objects that are grasped with power grasps. However, for the table tennis racket, four failed out of six initial viewpoints. Fig. 15 presents the objective value evolving

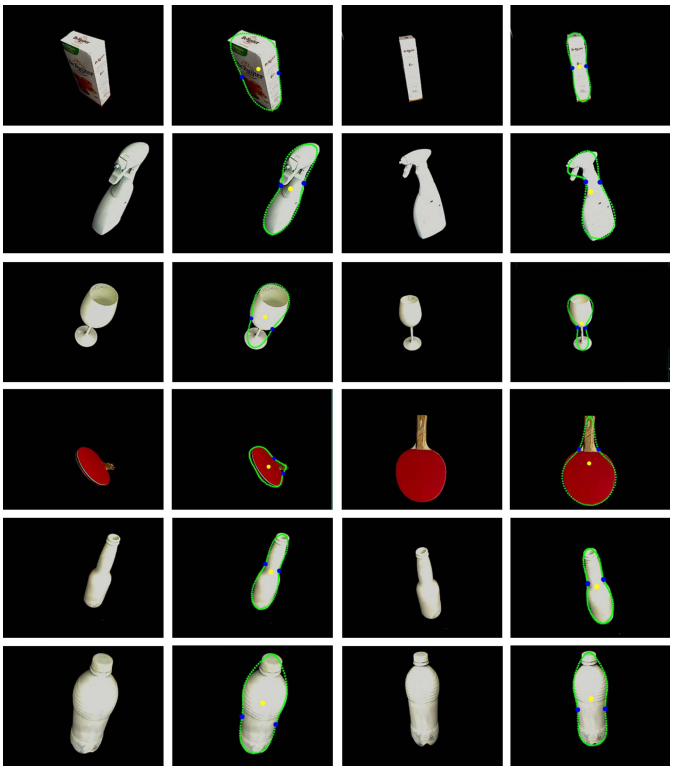

Fig. 14. Snapshots from the experiments. First and third columns are the initial views and the views obtained after the viewpoint optimization, respectively. Second and forth columns present the elliptic Fourier descriptors (EFD) model and synthesized grasping points for these views; the green points represent the EFD model, the yellow points are the centre of the models $[(a_0, c_0)$ points], and the blue points are the grasping points. Comparing the initial viewpoints with the final one, it can be seen that, the viewpoint optimization does not only help the grasping synthesis algorithm to generate better grasping points, but it also provides good approach vectors for the grasp execution.

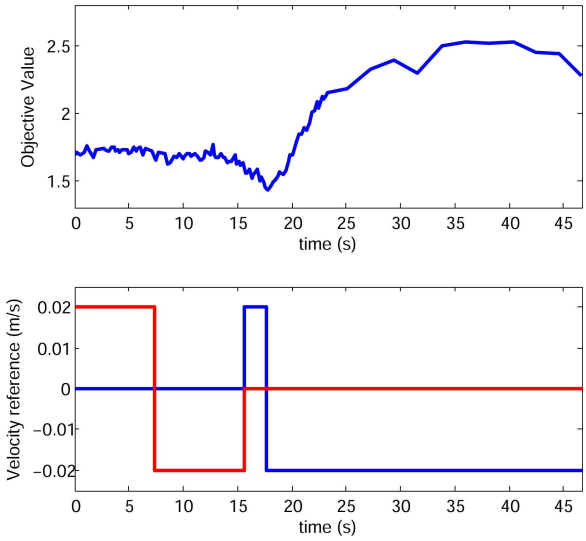

Fig. 15. Plots of the objective value and the velocity reference generated by the ESC algorithm for the spray bottle experiment that is presented in the second row of Fig. 14. In the velocity reference plot, the red and blue lines show the velocity references in the x- and y-directions, respectively.

in time and the generated velocity references for the spray bottle experiment whose snapshots are given in Fig. 14. These results are summarized in Table II.

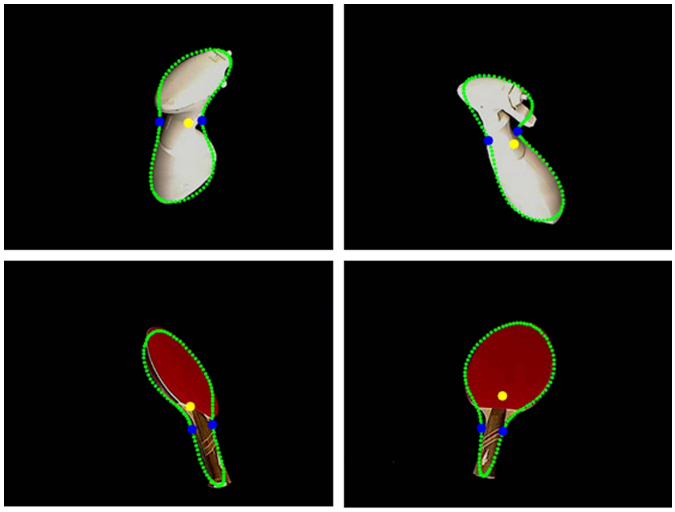

Fig. 16. Snapshots from the failed experiments. First column presents the initial views, and second column is the final views (both with EFD models). Green points are the EFD models, yellow points are the model centers, and blue points are the grasping points.

The failed spray bottle experiment and one example of the failed table tennis racket experiments are presented in Fig. 16. The reason of the failure for the spray bottle was that the optimizer overshot a better viewpoint because of the hysteresis mechanism. As a result the viewpoint became harder for grasping, and that led to failure. A solution of this would be to increase the signal-to-noise ratio and choose smaller hysteresis values. For the table tennis racket, although the viewpoint optimizer led the robot to a better viewpoint for grasping synthesis, the grasp still fails because the precision grasp brings the necessity for the fingers of the gripper to be aligned more precisely on the object.

V. Conclusion

In this paper, a novel viewpoint optimization methodology is proposed for robotic applications. Its model free and continuous characteristics provide flexibility and efficiency for the use of active vision in unstructured environments. We apply the methodology to active object recognition and grasping of unknown objects. In active object recognition, the model-free nature of the algorithm brings independence to offline data for the viewpoint optimization purposes. Therefore, unlike algorithms in literature, it can operate efficiently even when the offline data do not represent the situation at hand. Considering grasping of unknown objects, our methodology is the only one in the literature that can directly optimize a grasp success value.

The methodology treats the underlying algorithm as a black box. Therefore, applying it to algorithms and tasks other than the ones presented in this paper does not require any modification. The only necessity to enable such a viewpoint optimization is a success rate value supplied by the underlying algorithm. Nevertheless, depending on the properties and requirements of the task or the algorithm, another type of ESC method (e.g., perturbation-based ESC and approximation-based ESC; see [10]) can be utilized. In addition, the underlying algorithm should be fast enough to be run continuously (in 5–10 Hz) to maintain the efficiency. We also observed that having a high signal-to-noise ratio for the objective value boosts the performance of the viewpoint optimization procedure significantly as, e.g., for the case of NN-ESC, low hysteresis thresholds can be chosen.

ESC methods are local optimizers, and even though they have mechanisms for escaping the local optima, they may still get stuck in suboptimal states, e.g., some of the failed cases of our experiments. Combining the methodology with a higher level reasoning strategy, e.g., partially observable Markov decision processes [64], can increase its success significantly. In a recent study [28], a simplex-based strategy is also proposed to improve the global convergence performance of a particular ESC algorithm. While integrating this strategy would increase the convergence time, it can certainly be preferable in critical tasks.

References

[1] S. Chen, Y. Li, and N. M. Kwok, "Active vision in robotic systems: A survey of recent developments," *Int. J. Robot. Res.*, vol. 30, no. 11, pp. 1343–1377, 2011.

[2] M. F. Huber, T. Dencker, M. Roschani, and J. Beyerer, "Bayesian active object recognition via Gaussian process regression," in *Proc. 15th Int Inf. Fusion Conf. (FUSION)*, 2012, pp. 1718–1725.

[3] F. Deinzer, C. Derichs, H. Niemann, and J. Denzler, "A framework for actively selecting viewpoints in object recognition," *Int. J. Pattern Recognit. Artif. Intell.*, vol. 23, no. 4, pp. 765–799, 2009.

[4] S. Frintrop and P. Jensfelt, "Attentional landmarks and active gaze control for visual SLAM," *IEEE Trans. Robot.*, vol. 24, no. 5, pp. 1054–1065, Oct. 2008.

[5] G. Zhang, S. Ferrari, and M. Qian, "An information roadmap method for robotic sensor path planning," *J. Intell. Robot. Syst.*, vol. 56, nos. 1–2, pp. 69–98, 2009.

[6] M. Chessa, S. Murgia, L. Nardelli, S. P. Sabatini, and F. Solari, "Bio-inspired active vision for obstacle avoidance," in *Proc. Int. Conf. Comput. Graph. Theory Appl. (GRAPP)*, 2014, pp. 1–8.

[7] Y. F. Li and Z. G. Liu, "Information entropy-based viewpoint planning for 3-D object reconstruction," *IEEE Trans. Robot.*, vol. 21, no. 3, pp. 324–337, Jun. 2005.

[8] J. Delmerico, S. Isler, R. Sabzevari, and D. Scaramuzza, "A comparison of volumetric information gain metrics for active 3D object reconstruction," *Auto. Robots*, vol. 42, no. 2, pp. 197–208, 2018.

[9] Y. Motai and A. Kosaka, "Hand–eye calibration applied to viewpoint selection for robotic vision," *IEEE Trans. Ind. Electron.*, vol. 55, no. 10, pp. 3731–3741, Oct. 2008.

[10] B. Calli, W. Caarls, P. Jonker, and M. Wisse, "Comparison of extremum seeking control algorithms for robotic applications," in *Proc. IEEE/RSJ Int. Conf. Intell. Robots Syst. (IROS)*, Oct. 2012, pp. 3195–3202.

[11] X. S. Zhou, D. Comaniciu, and A. Krishnan, "Conditional feature sensitivity: A unifying view on active recognition and feature selection," in *Proc. 9th IEEE Int. Comput. Vis. Conf.*, Oct. 2003, pp. 1502–1509.

[12] T. Arbel and F. P. Ferrie, "Entropy-based gaze planning," *Image Vis. Comput.*, vol. 19, no. 11, pp. 779–786, Sep. 2001.

[13] M. A. Sipe and D. Casasent, "Feature space trajectory methods for active computer vision," *IEEE Trans. Pattern Anal. Mach. Intell.*, vol. 24, no. 12, pp. 1634–1643, Dec. 2002.

[14] J. Denzler and C. M. Brown, "Information theoretic sensor data selection for active object recognition and state estimation," *IEEE Trans. Pattern Anal. Mach. Intell.*, vol. 24, no. 2, pp. 145–157, Feb. 2002.

[15] C. Laporte, R. Brooks, and T. Arbel, "A fast discriminant approach to active object recognition and pose estimation," in *Proc. 17th Int. Conf. Pattern Recognit.*, vol. 3, 2004, pp. 91–94.

[16] J. Defretin, J. Marzat, and H. Piet-Lahanier, "Learning viewpoint planning in active recognition on a small sampling budget: A Kriging approach," in *Proc. 9th Int. Conf. Mach. Learn. Appl.*, 2010, pp. 169–174.

[17] A. Saxena, J. Driemeyer, and A. Y. Ng, "Robotic grasping of novel objects using vision," *Int. J. Robot. Res.*, vol. 27, no. 2, pp. 157–173, 2008.

[18] J. Bohg and D. Kragic, "Learning grasping points with shape context," *Robot. Auto. Syst.*, vol. 58, no. 4, pp. 362–377, 2010.

[19] Y. Jiang, S. Moseson, and A. Saxena, "Efficient grasping from rgbd images: Learning using a new rectangle representation," in *Proc. IEEE Int. Conf. Robot. Autom. (ICRA)*, May 2011, pp. 3304–3311.

[20] K. Hsiao, S. Chitta, M. Ciocarlie, and E. G. Jones, "Contact-reactive grasping of objects with partial shape information," in *Proc. IEEE/RSJ Int. Conf. Intell. Robots Syst. (IROS)*, Oct. 2010, pp. 1228–1235.

[21] S. Dragiev, M. Toussaint, and M. Gienger, "Gaussian process implicit surfaces for shape estimation and grasping," in *Proc. IEEE Int. Conf. Robot. Autom. (ICRA)*, May 2011, pp. 2845–2850.

[22] D. Holz *et al.*, *Active Recognition and Manipulation for Mobile Robot Bin Picking*. Cham, Switzerland: Springer, 2014, pp. 133–153. [Online]. Available: http://dx.doi.org/10.1007/978-3-319-03838-4_7

[23] L. P. Kaelbling and T. Lozano-Pérez, "Integrated task and motion planning in belief space," *Int. J. Robot. Res.*, vol. 32, nos. 9–10, pp. 1194–1227, 2013.

[24] J. Aleotti, D. L. Rizzini, and S. Caselli, "Perception and grasping of object parts from active robot exploration," *J. Intell. Robot. Syst.*, vol. 76, no. 3, pp. 401–425, 2014.

[25] G. Kahn *et al.*, "Active exploration using trajectory optimization for robotic grasping in the presence of occlusions," in *Proc. IEEE Int. Conf. Robot. Autom. (ICRA)*, May 2015, pp. 4783–4790.

[26] E. Arruda, J. Wyatt, and M. Kopicki, "Active vision for dexterous grasping of novel objects," in *Proc. IEEE/RSJ Int. Conf. Intell. Robots Syst. (IROS)*, Oct. 2016, pp. 2881–2888.

[27] Y. Zhang, J. Shen, M. Rotea, and N. Gans, "Robots looking for interesting things: Extremum seeking control on saliency maps," in *Proc. IEEE/RSJ Int. Conf. Intell. Robots Syst. (IROS)*, Sep. 2011, pp. 1180–1186.

[28] Y. Zhang, M. Rotea, and N. Gans, "Simplex guided extremum seeking control with convergence detection to improve global performance," *IEEE Trans. Control Syst. Technol.*, vol. 24, no. 4, pp. 1266–1278, Jul. 2016.

[29] N. J. Killingsworth, S. M. Aceves, D. L. Flowers, and M. Krstic, "Extremum seeking tuning of an experimental HCCI engine combustion timing controller," in *Proc. Amer. Control Conf. (ACC)*, 2007, pp. 3665–3670.

[30] W. R. Hsin-Hsiung, M. Krstic, and G. Bastin, "Optimizing bioreactors by extremum seeking," *Int. J. Adapt. Control Signal Process*, vol. 13, no. 651, pp. 651–669, 1999.

[31] S. Drakunov, U. Ozguner, P. Dix, and B. Ashrafi, "ABS control using optimum search via sliding modes," *IEEE Trans. Control Syst. Technol.*, vol. 3, no. 1, pp. 79–85, Mar. 1995.

[32] S. K. Korovin and V. I. Utkin, "Using sliding modes in static optimization and nonlinear programming," *Automatica*, vol. 10, no. 5, pp. 525–532, 1974.

[33] M. C. M. Teixeira and S. H. Zak, "Analog neural nonderivative optimizers," *IEEE Trans. Neural Netw.*, vol. 9, no. 4, pp. 629–638, Jul. 1998.

[34] C. Zhang and R. Ordonez, "Non-gradient extremum seeking control of feedback linearizable systems with application to ABS design," in *Proc. CDC*, 2006, pp. 6666–6671.

[35] K. B. Ariyur and M. Krstic, *Real-Time Optimization by Extremum-Seeking Control*. Wiley, 2003.

[36] J. I. Vásquez-Gómez, E. Löpez-Damian, and L. E. Sucar, "View planning for 3d object reconstruction," in *Proc. IEEE/RSJ Int. Conf. Intell. Robots Syst.*, Oct. 2009, pp. 4015–4020.

[37] D. Den Hertog, C. Roos, and T. Terlaky, "On the classical logarithmic barrier function method for a class of smooth convex programming problems," *J. Optim. Theory Appl.*, vol. 73, no. 1, pp. 1–25, 1992.

[38] S. Ekvall, P. Jensfelt, and D. Kragic, "Integrating active mobile robot object recognition and slam in natural environments," in *Proc. IEEE/RSJ Int. Intell. Robots Syst. Conf.*, Oct. 2006, pp. 5792–5797.

[39] D. Kragic, M. Björkman, H. I. Christensen, and J.-O. Eklundh, "Vision for robotic object manipulation in domestic settings," *Robot. Auto. Syst.*, vol. 52, no. 1, pp. 85–100, 2005.

[40] R. B. Rusu, Z. C. Marton, N. Blodow, M. Dolha, and M. Beetz, "Towards 3D point cloud based object maps for household environments," *Robot. Auto. Syst. J.*, vol. 56, no. 11, pp. 927–941, 2008.

[41] S. Vasudevan, S. Gächter, V. Nguyen, and R. Siegwart, "Cognitive maps for mobile robots—An object based approach," *Robot. Auto. Syst.*, vol. 55, no. 5, pp. 359–371, 2007.

[42] S. D. Roy, S. Chaudhury, and S. Banerjee, "Active recognition through next view planning: A survey," *Pattern Recognit.*, vol. 37, no. 3, pp. 429–446, 2004.

[43] G. de Croon, I. Sprinkhuizen-Kuyper, and E. Postma, "Comparing active vision models," *Image Vis. Comput.*, vol. 27, no. 4, pp. 374–384, 2009.

[44] H. Borotschnig, L. Paletta, M. Prantl, and A. Pinz, "Appearance-based active object recognition," *Image Vis. Comput.*, vol. 18, no. 9, pp. 715–727, 2000.

[45] L. Paletta and A. Pinz, "Active object recognition by view integration and reinforcement learning," *Robot. Auto. Syst.*, vol. 31, nos. 1–2, pp. 71–86, 2000.

[46] K. Shibata, T. Nishino, and Y. Okabe, "Active perception and recognition learning system based on actor-q architecture," *Syst. Comput. Jpn.*, vol. 33, no. 14, pp. 12–22, 2002.

[47] E. Johns, S. Leutenegger, and A. J. Davison, "Pairwise decomposition of image sequences for active multi-view recognition," in *Proc. IEEE Conf. Comput. Vis. Pattern Recognit. (CVPR)*, Jun. 2016, pp. 3813–3822.

[48] H. Liu, F. Li, X. Xu, and F. Sun, "Active object recognition using hierarchical local-receptive-field-based extreme learning machine," in *Memetic Computing*. Berlin, Germany: Springer, 2017.

[49] M. Malmir, K. Sikka, D. Forster, J. Movellan, and G. W. Cottrell, "Deep Q-learning for active recognition of GERMS: Baseline performance on a standardized dataset for active learning," in *Proc. Brit. Mach. Vis. Conf. (BMVC)*, 2015, pp. 161-1–161-11.

[50] E. González, A. Adán, V. Feliú, and L. Sánchez, "Active object recognition based on Fourier descriptors clustering," *Pattern Recognit. Lett.*, vol. 29, no. 8, pp. 1060–1071, 2008.

[51] F. Farshidi, S. Sirouspour, and T. Kirubarajan, "Active multi-camera object recognition in presence of occlusion," in *Proc. IEEE/RSJ Int. Conf. Intell. Robots Syst. (IROS)*, Aug. 2005, pp. 2718–2723.

[52] K. Wu, R. Ranasinghe, and G. Dissanayake, "Active recognition and pose estimation of household objects in clutter," in *Proc. IEEE Int. Conf. Robot. Autom. (ICRA)*, May 2015, pp. 4230–4237.

[53] R. Eidenberger and J. Scharinger, "Active perception and scene modeling by planning with probabilistic 6D object poses," in *Proc. IEEE/RSJ Int. Intell. Robots Syst. Conf. (IROS)*, Oct. 2010, pp. 1036–1043.

[54] P. Robbel and D. Roy, "Exploiting feature dynamics for active object recognition," in *Proc. 11th Int. Control Autom. Robot. Vis. Conf. (ICARCV)*, 2010, pp. 2102–2108.

[55] R. Fergus, L. Fei-Fei, P. Perona, and A. Zisserman, "Learning object categories from Google's image search," in *Proc. 10th IEEE Int. Conf. Comput. Vis. (ICCV)*, vol. 2, Oct. 2005, pp. 1816–1823.

[56] E. Hidalgo-Peña, L. F. Marin-Urias, F. Montes-González, A. Marín-Hernández, and H. V. Ríos-Figueroa, "Learning from the Web: Recognition method based on object appearance from Internet images," in *Proc. 8th ACM/IEEE Int. Conf. Hum.-Robot Interact.*, Mar. 2013, pp. 139–140.

[57] A. Haasch, N. Hofemann, J. Fritsch, and G. Sagerer, "A multi-modal object attention system for a mobile robot," in *Proc. IEEE/RSJ Int. Conf. Intell. Robots Syst.*, Aug. 2005, pp. 2712–2717.

[58] C. Dance, J. Willamowski, L. Fan, C. Bray, and G. Csurka, "Visual categorization with bags of keypoints," in *Proc. ECCV Int. Workshop Stat. Learn. Comput. Vis.*, 2004, pp. 1–2.

[59] J. C. Platt, "Probabilistic outputs for support vector machines and comparisons to regularized likelihood methods," *Adv. Large Margin Classifiers*, vol. 10, no. 3, pp. 61–74, 1999.

[60] A. Saxena, J. Driemeyer, J. Kearns, C. Osondu, and A. Y. Ng, "Learning to grasp novel objects using vision," in *Proc. 10th Int. Symp. Experim. Robot.*, 2006, pp. 33–42.

[61] G. Recatalá, E. Chinellato, Á. P. del Pobil, Y. Mezouar, and P. Martinet, "Biologically-inspired 3D grasp synthesis based on visual exploration," *Auto. Robots*, vol. 25, nos. 1–2, pp. 59–70, 2008.

[62] B. Calli, M. Wisse, and P. Jonker, "Grasping of unknown objects via curvature maximization using active vision," in *Proc. IEEE/RSJ Int. Conf. Intell. Robots Syst. (IROS)*, Sep. 2011, pp. 995–1001.

[63] G. A. Kragten, "Underactuated hands: Fundamentals, performance analysis and design," Ph.D. dissertation, Faculty Mech., Maritime Mater. Eng., Delft Univ. Technol., Delft, The Netherlands, 2011.

[64] M. T. J. Spaan, *Partially Observable Markov Decision Processes*. Berlin, Germany: Springer, 2012, pp. 387–414.

Berk Calli (M'15) received the Bachelor of Science and Master of Science degrees in Mechatronics from Sabanci University, Istanbul, Turkey, with his thesis on integrated visual servoing and force control for robotic manipulation, and the Ph.D. degree from the Delft University of Technology, Delft, The Netherlands, in 2015 with his thesis on viewpoint optimization for improving grasp synthesis performance.

He is currently with the GRAB Laboratory, Yale University, New Haven, CT, USA, working on vision-based manipulation, dexterous manipulation, and manipulation benchmarking.

Wouter Caarls (S'03–M'12) received the M.Sc. (Hons.) degree in artificial intelligence from the University of Amsterdam, Amsterdam, The Netherlands, and the Ph.D. degree from the Delft University of Technology, Delft, The Netherlands, on the subject of the automatic optimization of a parallel computer architecture for smart cameras.

He is currently an Assistant Professor with the Department of Electrical Engineering, Pontifical Catholic University of Rio de Janeiro, Rio de Janeiro, Brazil, investigating the applications of reinforcement learning in robotics. His research interests include robotics, machine learning, optimization, parallel algorithms, and image processing.

Martijn Wisse (S'02–M'04) received the M.Sc. and Ph.D. degrees in mechanical engineering from the Delft University of Technology, Delft, The Netherlands.

He is currently a Full Professor with the Delft University of Technology. His previous research interests included passive dynamic walking robots. His current research interests include the field of robot manipulators for agile manufacturing, underactuated grasping, open-loop stable manipulator control, design of robotic arms and robotic systems, agile manufacturing, and the creation of start-up companies.

Pieter P. Jonker (M'91) received the M.Sc. degree in electrical engineering from the Twente University of Technology, Enschede, The Netherlands, in 1979, and the Ph.D. degree in physics from the Delft University of Technology (TUDelft), Delft, The Netherlands, in 1992.

He is currently a Full Professor of Vision-Based Robotics with the Bio-Mechanical Engineering Group, TUDelft. With Dr. M. Wisse, he runs the Dutch Bio-Robotics Laboratory, TUDelft. His current research interests include bioinspired real-time embedded vision systems for robotics, surveillance, and augmented reality, and on hierarchical reinforcement learning for walking robots.

Dr. Jonker is a Fellow of the IAPR.